Thrombin-Bound Conformation of the C-Terminal Fragments of Hirudin Determined by Transferred Nuclear Overhauser Effects†

Feng Ni* and Yasuo Konishi

Section of Protein Engineering, Biotechnology Research Institute, National Research Council Canada, Montrêal, Quêbec, Canada H4P 2R2

Harold A. Scheraga*

Baker Laboratory of Chemistry, Cornell University, Ithaca, New York 14853-1301

Received October 27, 1989; Revised Manuscript Received January 4, 1990

ABSTRACT: The interaction of the C-terminal fragments (residues 52–65 and 55–65) of the thrombin-specific inhibitor hirudin with bovine thrombin was studied by use of one- and two-dimensional NMR techniques in aqueous solution. Thrombin induces specific line broadening of the proton resonances of residues Asp(55) to Gln(65) of the synthetic hirudin fragments H-Asn-Asp-Gly-Asp(55)-Phe-Glu-Glu-Ile-Pro-Glu-Glu-Tyr(63)-Leu-Gln-COOH and acetyl-Asp(55)-Phe-Glu-Glu-Ile-Pro-Glu-Glu-Tyr(63)-Leu-Gln-COOH. This demonstrates that residues 55–65 are the predominant binding site of hirudin fragments with thrombin. Hirudin fragments take on a well-defined structure when bound to thrombin as indicated by several long-range *transferred* NOEs between the backbone and side-chain protons of the peptides, but they are not structured when free in solution. Particularly, transferred NOEs exist between the αCH proton of Glu(61) and the NH proton of Leu(64) [$d_{\alpha N}(i,i+3)$], between the αCH proton of Glu(61) and the βCH_2 protons of Leu(64) [$d_{\alpha\beta}(i,i+3)$], and between the αCH proton of Glu(62) and the γCH_2 protons of Gln(65) [$d_{\alpha\gamma}(i,i+3)$]. These NOEs are characteristic of an α-helical structure involving residues Glu(61) to Gln(65). There are also NOEs between the side-chain protons of residues Phe(56), Ile(59), Pro(60), Tyr(63), and Leu(64). Distance geometry calculations suggest that in the structure of the thrombin-bound hirudin peptides all the charged residues lie on the opposite side of a hydrophobic cluster formed by the nonpolar side chains of residues Phe(56), Ile(59), Pro(60), Tyr(63), and Leu(64).

Thrombin is a key enzyme in blood coagulation and interacts with many components of the coagulation cascade (Fenton, 1981). It converts the circulating fibrinogen to the fibrin clot. It amplifies its own generation by activating clotting factors V and VIII. It stimulates platelet aggregation and activates the fibrin cross-linking factor XIII. After clot formation, thrombin is inactivated by circulating inhibitors such as the antithrombin III–heparin complex. Thrombin can also be inhibited by low molecular weight molecules constructed on the basis of its substrate specificity (Kettner & Shaw, 1979; Stürzebecher et al., 1983; Kikumoto et al., 1984). These inhibitors have been tested for the control of thrombosis in experimental models and in humans (Kaiser et al., 1985; Kobayashi et al., 1987).

Hirudin is a small protein of 65 amino acid residues found in the salivary glands of medicinal leeches (Markwardt, 1970; Badgy et al., 1976; Dodt et al., 1984). It is a very potent anticoagulant with very little effect in other biological pathways in the blood (Markwardt et al., 1982; Gilboa et al., 1988). Hirudin exhibits its anticoagulant activity by the formation of a tight complex with α-thrombin ($K_{diss} \sim 10^{-14}$ M), thereby preventing the thrombin-catalyzed conversion of fibrinogen to the fibrin clot (Markwardt, 1970; Stone & Hofsteenge, 1986). The binding of hirudin also prevents thrombin from activating factors V, VIII, and XIII and platelets (Fenton, 1981). These unique properties of hirudin have promoted considerable interest in its potential use as an antithrombotic agent (Walsmann & Markwardt, 1981; Markwardt et al., 1982, 1988).

Recently, a significant amount of information has been accumulated concerning the mechanism of thrombin inhibition by hirudin. The solution structures of natural and recombinant hirudins have been investigated by using two-dimensional NMR[1] methods (Sukumaran et al., 1987; Clore et al., 1987; Folkers et al., 1989; Haruyama & Wüthrich, 1989; Haruyama et al., 1989). It was found that hirudin has a disulfide-linked core structure (residues 1–48) and a largely unstructured C-terminal region from residue 49 to 65. The tight binding of hirudin to thrombin appears to be a result of very complex interactions, possibly involving multiple contact sites between the two molecules (Fenton, 1981; Chang, 1986, 1989; Stone & Hofsteenge, 1986; Stone et al., 1987). The action of hirudin does not seem to conform to the standard mechanism of action of serine protease inhibitors (Laskowski & Kato, 1980) since none of the positively charged residues in hirudin have been identified to interact specifically with the active site of thrombin (Dodt et al., 1988; Braun et al., 1988; Degryse et al., 1989). The C-terminal region of hirudin, on the other hand, may play an important role in the interaction. This is

† NRCC Pulication No. 30971. This investigation was supported in part by NIH Grants GM-24893 and HL-30616.

[1] Abbreviations: NMR, nuclear magnetic resonance; NOE, nuclear Overhauser effect; DQF-COSY, double-quantum-filtered coherence-transfer spectroscopy; Relayed-COSY, relayed coherence-transfer spectroscopy; TOCSY, total coherence-transfer spectroscopy; ROESY, rotating-frame nuclear Overhauser and exchange spectroscopy; NOESY, two-dimensional nuclear Overhauser and exchange spectroscopy; FID, free induction decay; EDTA, ethylenediaminetetraacetic acid; Fmoc, N^{α}-[[(9-fluorenylmethyl)oxy]carbonyl]; *t*-BOC, *tert*-butyloxycarbonyl; PEG 6000, poly(ethylene glycol) with an average molecular weight of 6000; FPLC, fast protein liquid chromatography; RPLC, reverse-phase high-performance liquid chromatography; SDS–PAGE, sodium dodecyl sulfate–polyacrylamide gel electrophoresis; TFA, trifluoroacetic acid; PPACK, D-Phe-Pro-arginine chloromethyl ketone.

0006-2960/90/0429-4479$02.50/0

HR1

```
    52  53  54  55  56  57  58  59  60  61  62  63  64  65
H-Asn-Asp-Gly-Asp-Phe-Glu-Glu-Ile-Pro-Glu-Glu-Tyr-Leu-Gln-COOH
```

HR2

```
                55  56  57  58  59  60  61  62  63  64  65
Acetyl-Asp-Phe-Glu-Glu-Ile-Pro-Glu-Glu-Tyr-Leu-Gln-COOH
```

FIGURE 1: Amino acid sequences of peptides derived from the C-terminal region of desulfohirudin. Peptide HR1 has a free N-terminus, and the N-terminus of peptide HR2 is blocked with an acetyl group to remove end charge effects.

supported by the observation that desulfonation of natural hirudin at Tyr(63) resulted in reduced thrombin binding (Chang, 1983; Braun et al., 1988). Proteolytic removal of the C-terminal residues also resulted in significant loss of the inhibitory activity of hirudin (Chang, 1983; Dodt et al., 1987). Kinetic analysis showed that the tight binding between hirudin and thrombin arises from the combination of a slow rate of dissociation and a fast rate of association that can be reduced significantly by mutations of Glu(57), Glu(58), Glu(61), and Glu(62) of hirudin to noncharged glutamine residues (Stone & Hofsteegne, 1986; Stone et al., 1987; Braun et al., 1988). The importance of residues 55–65 of hirudin was further demonstrated by the finding that the thrombin-induced polymerization of fibrinogen can be inhibited by synthetic peptides derived from this 11-residue fragment (Krstenansky et al., 1987; Mao et al., 1988). These hirudin peptides do not inhibit the thrombin-catalyzed proteolysis of tripeptide chromogenic substrates, indicating that the C-terminal region of hirudin may bind to a noncatalytic site of thrombin that is involved in the interaction with fibrinogen.

In our previous studies, we employed NMR techniques to determine the thrombin-bound conformation of human fibrinopeptide A and provided a structural basis for the specificity of the interaction of thrombin with fibrinogen (Ni et al., 1989a–c). In the present work, we have applied the high-resolution NMR methods to study the interaction of thrombin with two peptides that correspond to residues 52–65 and residues 55–65 of hirudin. A comparison of the NMR data of the two peptides further established that residues 55–65 are the predominant binding site in the interaction with thrombin. Most importantly, measurements of transferred nuclear Overhauser effects have enabled us to define the structure of the last 10 residues of hirudin in the thrombin–peptide complex.

Experimental Procedures

Peptide Synthesis and Purification. The peptides HR1 and HR2 (Figure 1), derived from the C-terminal residues of desulfohirudin, were prepared by using Fmoc and *t*-BOC amino acids, respectively, by the solid-phase method described elsewhere (Konishi et al., 1989). The peptides were purified on a semipreparative RPLC column (C_{18}, Vydac) with a 2–60% acetonitrile gradient in water in the presence of 0.1% TFA.

The thrombin-specific inhibitor D-Phe-Pro-arginine chloromethyl ketone (PPACK) was purchased from CalBiochem and used without further purification.

Preparation of Bovine Thrombin. Bovine thrombin was obtained from bovine plasma barium citrate eluate (Sigma) according to a procedure described previously (Ni et al., 1989b) with the following modifications. In order to minimize the formation of β-thrombin, prothrombin was activated only for 30 min at 37 °C. Purification of thrombin was carried out on a Mono-S HR 10/10 (Pharmacia) cation-exchange column using a salt gradient of 0.1–0.7 M NaCl in 25 mM sodium phosphate at pH 6.5 delivered by a Pharmacia FPLC system. The pools containing thrombin were identified by clotting assay (Lundblad, 1971) using bovine fibrinogen (Sigma, Type I-S). Pooled thrombin was characterized by reducing SDS–PAGE on a PhastGel system (Pharmacia). Both silver and Coomassie blue staining of the gel identified one major band (>90%) corresponding to the intact B-chain of α-thrombin. The shorter activation time reduced the minor bands corresponding to the molecular weights of the fragmented B-chain of thrombin (β-thrombin). Purified thrombin was stored at 0 °C in 25 mM sodium phosphate buffer containing ~350 mM NaCl at pH 6.5. No decomposition was observed for the protein during storage as judged by SDS–PAGE and by a constant UV absorption of the solution. A concentrated solution of thrombin was prepared by solvent exchange into a buffer that was 150 mM in NaCl, 50 mM in sodium phosphate, and 0.2 mM in EDTA at pH 5.3, employing a CentriCon (Amicon) apparatus with a molecular weight cutoff of 10000. The concentrated thrombin solution was used immediately for NMR measurements. The final thrombin concentration was determined by its absorbance, using the value of $E_{280}^{1\%} = 19.5$ (Winzor & Scheraga, 1964).

NMR Sample Preparation. The preparation of NMR samples involved the following steps. The hirudin peptides (3–7 mg) were dissolved in 0.5 mL of deionized water. The pH of the solutions was adjusted to 5.3 with trace amounts of dilute HCl or NaOH. The peptide solutions were then dried under vacuum on a SpeedVac system (Savant). For NMR samples of the free peptides, the dried peptides were taken up in 450 μL of an H_2O solution that was 50 mM in sodium phosphate, 150 mM in NaCl, and 0.2 mM in EDTA at pH 5.3 and 50 μL of a corresponding D_2O solution. For samples of the thrombin–peptide complexes, the dried peptides were dissolved in 450 μL of the concentrated thrombin solution and 50 μL of the D_2O solution at pD 5.3. The pH of the final solutions were 5.3 ± 0.1.

NMR Measurements. NMR experiments were carried out on a Brüker AM-500 spectrometer. Spectral analysis and plotting were carried out on a Brüker Aspect 3000 workstation and/or on a MicroVax 3500/VMS computer using the FT NMR program provided by Dr. Dennis Hare (Hare Research Inc., Seattle, WA). All one-dimensional data were processed without any apodization.

All of the two-dimensional spectra of the peptides were acquired in the phase-sensitive mode (Aue et al., 1976) employing time-proportional phase incrementation (Redfield & Kuntz, 1975) along the t_1 direction (Marion & Wüthrich, 1983; Bodenhausen et al., 1984a). To avoid excitation of the solvent, the carrier frequency was placed at the position of the water proton resonance, and the observation pulse was replaced by the jump-return sequence (Plateau & Guéron, 1982) with a delay of 0.200 ms. Alternatively, a selective saturation pulse with the frequency of the water proton resonance was turned on during the relaxation delay and during evolution and mixing (Wider et al., 1983, 1984). Phase-sensitive DQF-COSY spectra were acquired by using the procedure of *ZZ*-coherence transfer (Bodenhausen et al., 1984b; Zuiderweg, 1987). Procedures for the following experiments were described previously with modifications discussed in the more recent references: Relayed-COSY with a mixing time τ_m of 36 ms (Eich et al., 1982; Wagner, 1983), TOCSY with $\tau_m = 70$ ms (Braunschweiler & Ernst, 1983; Bax & Davis, 1985b; Rance, 1987), and ROESY with $\tau_m = 115$ ms (Bothner-By et al., 1984; Bax & Davis, 1985a; Kessler et al., 1987; Rance, 1987).

For NOESY spectra (Jeener et al., 1979; Macura & Ernst, 1980), a procedure for t_1-ridge suppression was employed to

Table I: Proton Resonance Assignments of Hirudin Fragments at 25 °C and pH 5.3

residue	chemical shift (ppm) NH	αCH	βCH	others
			Peptide HR1	
N52		4.38	2.96, 3.00	δNH_2 7.00, 7.73
D53	8.86	4.63	2.64, 2.76	
G54	8.48	3.87, 3.99		
D55	8.03	4.57	2.61, 2.61	
F56	8.19	4.61	3.04, 3.16	δCH_2 7.25; ϵCH_2 7.36; ζCH 7.31
E57	8.18	4.27	1.89, 2.00	γCH_2 2.26, 2.26
E58	8.32	4.28	1.93, 2.02	γCH_2 2.28, 2.28
I59	8.26	4.45	1.86	γCH_2 1.16, 1.51; γCH_3 0.94; δCH_3 0.84
P60		4.39	1.87, 2.31	γCH_2 1.97, 2.02; δCH_2 3.65, 3.89
E61	8.46	4.16	1.97, 1.97	γCH_2 2.34, 2.34
E62	8.45	4.22	1.92, 1.92	γCH_2 2.16, 2.16
Y63	8.13	4.63	2.94, 3.12	δCH_2 7.12; ϵCH_2 6.83
L64	8.04	4.36	1.62, 1.62	γCH 1.53; δCH_3 0.84, 0.90
Q65	7.76	4.15	1.93, 2.13	γCH_2 2.29, 2.29; ϵNH_2 6.80, 7.50
			Peptide HR2	
D55	8.18	4.54	2.49, 2.61	
F56	8.16	4.63	3.03, 3.19	δCH_2 7.27; ϵCH_2 7.37; ζCH 7.32
E57	8.24	4.29	1.91, 2.04	γCH_2 2.27, 2.27
E58	8.34	4.31	1.94, 2.05	γCH_2 2.29, 2.29
I59	8.28	4.44	1.87	γCH_2 1.16, 1.51; γCH_3 0.96; δCH_3 0.85
P60		4.40	1.87, 2.33	γCH_2 1.98, 2.02; δCH_2 3.65, 3.88
E61	8.48	4.16	1.98, 1.98	γCH_2 2.34, 2.34
E62	8.47	4.23	1.92, 1.92	γCH_2 2.17, 2.17
Y63	8.13	4.62	2.95, 3.14	δCH_2 7.13; ϵCH_2 6.84
L64	8.03	4.37	1.62, 1.62	γCH 1.53; δCH_3 0.85, 0.91
Q65	7.77	4.14	1.93, 2.14	γCH_2 2.31, 2.31; ϵNH_2 6.81, 7.51

improve spectral clarity (sine-modulated NOESY; Otting et al., 1986). Proper cycling of the phases of the radio-frequency (rf) transmitter and receiver was also adopted for the suppression of multiple quantum coherences (except for zero quantum) and other spectrometer artifacts (Wider et al., 1984). Postacquisition delay was set to a value of 1.5 s for a more complete magnetization recovery. Typically, 64–160 accumulations were collected for each FID of 2K data points. A total of 300–512 FIDs were collected for the two-dimensional data matrix. The FID matrices were all premultiplied by a 22.5°-shifted sine bell in the t_1 direction and a 45°-shifted sine bell in the t_2 direction before Fourier transformation.

Distance Geometry Calculations. For the calculation of the three-dimensional structure of the thrombin-bound peptide, upper bounds and some lower bounds of the interproton distances were estimated from NOE cross-peaks in a NOESY spectrum (200 ms mixing time) of peptide HR2 interacting with thrombin. Another NOESY spectrum with a mixing time of 100 ms was used to check for the possible existence of spin diffusion. The relative intensities of the NOE cross-peaks were classified into three categories, weak (w), medium (m), or strong (s), by counting the number of contour levels for each peak (Wüthrich, 1986). The sizes of the contours of some very broad NOE cross-peaks were also taken into account in the classification. For example, an NOE peak of medium intensity was reclassified as strong if the diameter of the contour was much larger than that of the average contours. In some cases, where there were local distortions of the spectral base plane, one-dimensional projections of selected spectral regions were used to compare peak intensities following the practice outlined in our previous paper (Ni et al., 1989a).

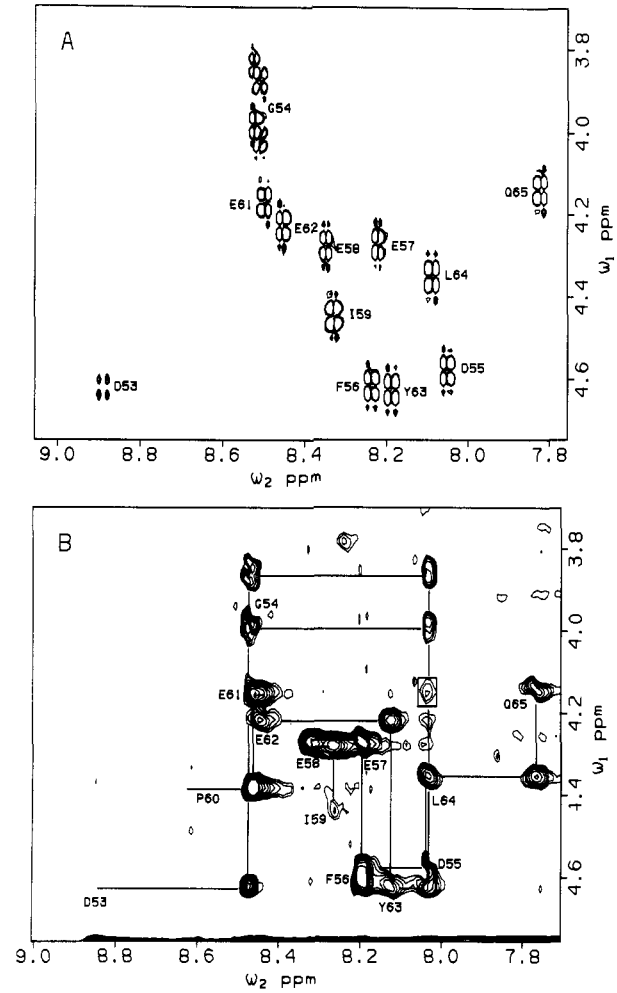

FIGURE 2: (A) The fingerprint region of a DQF-COSY spectrum of an 8 mM solution of peptide HR1 at 20 °C (Figure 1). Assignments are made to individual residues as discussed in the text. (B) Sequential αCH–NH NOE connectivities derived from a two-dimensional NOE spectrum of peptide HR1 acquired at 25 °C in the presence of thrombin. The NMR solution contained 8 mM peptide HR1 and 0.5 mM bovine thrombin. The boxed area indicates a weak NOE connectivity between the αCH proton of Glu(61) and the NH proton of Leu(64) (see later sections).

Distance geometry computations were carried out on a MicroVax 3500/VMS computer or on an Intel parallel computer (iPSC/2) using an implementation (Vâsquez & Scheraga, 1988; Ni et al., 1989c) of a variable-target-function procedure (Braun & Gō, 1985). Calculations of structure were carried out in an iterative manner. This involved computing a set of initial structures by using distance constraints derived from well-resolved transferred NOEs. These initial structures provided information for the identification of additional NOEs, particularly those with low intensity and those with chemical shift degeneracy. Lower bounds between some protons were also identified if an NOE cross-peak was not observed between two protons that were less than 4.0 Å apart in the computed structures. A new set of structures were then generated incorporating distance constraints that contained the newly identified ones. The computed structures were displayed and compared on an Evans & Sutherland PS390 computer graphics system with the programs HYDRA (Polygen) and FRODO (Rice University).

Results

Assignments of Proton Resonances and Confirmation of Peptide Sequences. Sequence-specific assignments (Figure 2A and Table I) of the backbone proton (NH and αCH)

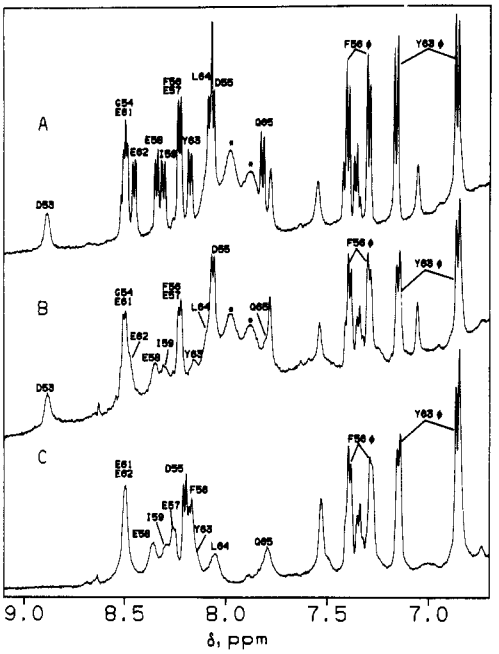

FIGURE 3: NH and aromatic regions of the proton spectra of peptides HR1 and HR2 in H_2O at 25 °C: (A) an 8 mM solution of peptide HR1; (B) an 8 mM solution of peptide HR1 in the presence of 0.5 mM bovine thrombin; (C) a 10 mM solution of peptide HR2 in the presence of 0.36 mM bovine thrombin. All of the NH peaks are labeled with the corresponding residues (Figure 1). The letter ϕ indicates that these peaks are from the ring protons of Phe(56) and Tyr(63). The asterisks in traces A and B identify resonance peaks arising from small scavenger molecules copurified with peptide HR1. They are absent in peptide HR2 (trace C).

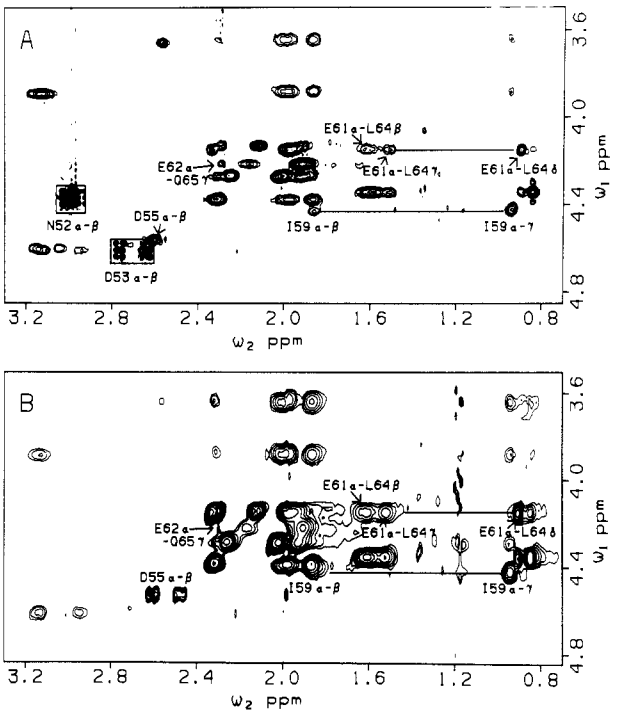

FIGURE 4: αCH–βCH and aliphatic regions of the two-dimensional NOE spectra of peptides HR1 (A) and HR2 (B) in the presence of bovine thrombin at pH 5.3. The concentrations of peptide HR1 and HR2 were 4 and 10 mM, respectively. The concentration of thrombin was 0.26 mM for the HR1 sample (A) and 0.36 mM for the HR2 sample (B). The NOESY spectra were acquired with a mixing time of 200 ms at 25 °C. The boxed cross-peaks are from the interactions (zero-quantum coherence or NOE) between the αCH and βCH_2 protons of residues Asn(52), Asp(53), and Asp(55). Also indicated are the medium-range NOEs between the αCH proton of Glu(61) and the side-chain protons of Leu(64) and between the αCH proton of Glu(62) and the γCH_2 protons of Gln(65). Identification of the NOEs between residues Glu(61) and Leu(64) is unambiguous since the αCH protons of Glu(61) and Gln(65) are clearly resolved from each other in both hirudin peptides (Figure 2A and Table I). The NOE between the αCH proton of Glu(62) and the γCH_2 protons of Gln(65) in the spectrum of HR2 (B) has a distorted shape due to local irregularities of the spectral base plane. The shape of this cross-peak is similar to that for HR1 (A) in the same spectral region above the diagonal (not shown).

resonances of peptides HR1 and HR2 in aqueous solutions at pH 5.3 were established on the basis of a combined analysis of the DQF-COSY and NOESY/ROESY spectra of these peptides according to a method described previously (Wüthrich, 1986). Further assignments of the side-chain proton resonances of each residue were made by a comparison of the Relayed-COSY and TOCSY spectra of these peptides. The tracings of the sequential NOE connectivities of backbone protons (Figure 2B) were found to be unique, indicating that these synthetic peptides have the correct sequences corresponding to the C-terminal region of desulfohirudin (Dodt et al., 1984).

As seen in Table I, there is general agreement between the proton chemical shifts of the free peptides HR1 and HR2. This is especially true for the chemical shifts of the αCH, βCH, and other side-chain protons. The chemical shifts of these protons in the free peptides are also very close to the chemical shifts of those residues in recombinant desulfohirudins reported recently (Folkers et al., 1989; Haruyama & Wüthrich, 1989). The exceptions are residues Asn(52), Asp(53), and Gly(54) in peptide HR1. The deviation of the proton chemical shifts of these residues can be explained by the induction effect of the positively charged free N-terminus present in peptide HR1, as observed in our previous NMR studies of fibrinogen-like peptides (Ni et al., 1988). The small differences in the chemical shifts of the NH protons, which are sensitive to pH change, are due to the pH differences of the peptide solutions used in this study (pH 5.3) and the protein solutions in the study of recombinant desulfohirudins (pH 3.0–4.5) (Folkers et al., 1989; Haruyama & Wüthrich, 1989).

Thrombin-Induced Line Broadening in Hirudin Peptides. Figure 3 shows the NH and aromatic regions of the proton spectra of peptide HR1 free in solution and peptides HR1 and HR2 in the presence of thrombin. Some resonance peaks from the peptides are significantly affected by thrombin binding. By a comparison of spectra A and B, Figure 3, we can easily identify broadened NH resonances from residues Glu(58), Ile(59), Glu(62), Tyr(63), Leu(64), and Gln(65). The NH protons of Asp(53), Gly(54) [and/or Glu(61)] and Asp(55), on the other hand, are much less affected by thrombin binding. The NH proton resonances of Glu(57) is also broadened by thrombin as seen from the spectra of peptide HR2 (Figure 3C) where the removal of residues Asn(52), Asp(53), and Gly(54) results in a separation of the overlapped NH resonances of residues Phe(56) and Glu(57) in peptide HR1 (Figure 3A,C). It is also seen that the NH proton of Phe(56) is broadened to a lesser extent than that of Glu(57). With this truncated peptide, peaks around 8.48 ppm arise from the resonances of the NH protons of only Glu(61) and Glu(62) (Figure 3C). The relatively intense peak at this position can be attributed largely to that of the NH proton of residue Glu(61), since the resonance of Glu(62) should be significantly attenuated by the presence of thrombin (Figure 3B).

The side-chain proton resonances of the hirudin peptides are also affected by thrombin binding. All of the ring protons of residues Phe(56) and Tyr(63) are broadened in the presence of thrombin (Figure 3). Figure 4A shows the aliphatic region of a two-dimensional spectrum (*J* correlation + cross relax-

ation) of peptide HR1 interacting with thrombin. In this spectrum, only the αCH–βCH interactions of residues Asn(52) and Asp(53) give rise to well-resolved multiplets characteristic of coherence transfer between *J*-coupled protons (Figure 2A) (Bodenhausen et al., 1984b). All other residues exhibit broad cross-peaks between their αCH and side-chain protons regardless of the existence of the through-bond *J* coupling or not, as is the case for all residues in the shorter peptide HR2 shown in Figure 4B. These broad cross-peaks indicate that the relaxation behavior of the side-chain protons of residues Asp(55) to Gln(65) is significantly affected by thrombin binding, since similar spectra of free peptides HR1 and HR2 contain only cross-peaks due to coherence transfer between coupled protons (spectra not shown).

We also acquired spectra of hirudin peptides in the presence of a modified thrombin whose clotting activity was completely abolished by the irreversible thrombin inhibitor D-Phe-Pro-arginine chloromethyl ketone (PPACK) (Kettner & Shaw, 1979). Thrombin-induced line broadening persists in these spectra. Furthermore, all the cross-peaks in the spectrum of HR2 interacting with the derivatized thrombin were identical with those seen in the spectrum of HR2 interacting with active thrombin (Figure 4B).

Transferred NOEs of Thrombin-Bound Hirudin Peptides. At room temperature, both of the hirudin-derived peptides exhibit very few NOEs in aqueous solutions even with a very long mixing time of 500 ms (spectra not shown). In a ROESY experiment in which cross relaxation between protons becomes much more efficient for medium-sized molecules (Bothner-By et al., 1984; Bax & Davis, 1985a), no NOEs other than those arising from sequential interactions were observed for the free peptide, HR1 in solution at 20 °C (spectra not shown). This is in agreement with the previous finding that no medium- or long-range NOEs exist in the C-terminal region of the intact hirudin molecule (Sukumaran et al., 1987; Clore et al., 1987; Folkers et al., 1989; Haruyama & Wüthrich, 1989).

In the NOESY spectra of the hirudin peptides with a large molar excess (>10-fold) over that of thrombin, numerous NOE cross-peaks can be seen at 25 °C even with a mixing time of 200 ms (Figures 4 and 5). Thus, the exchange rates of the hirudin peptides between the free and the thrombin-bound states are such that the peptides in the free state carry specific information about proton relaxation of the bound peptides (Albrand et al., 1979; Clore & Gronenborn, 1982). In the NOESY spectra of peptides interacting with thrombin, four kinds of cross-peaks may exist: (a) coherence-transfer peaks between protons whose relaxation behavior is not affected by thrombin binding; (b) NOEs originating from the protons of the bound peptide (intramolecular transferred NOEs; Albrand et al., 1979; Clore & Gronenborn, 1982); (c) NOEs between the protons of the bound peptide and the protons on the enzyme surface (intermolecular transferred NOEs; Balaram et al., 1972; James, 1976); and (d) NOEs between protons on the enzyme. Peaks a above due to coherence transfers are easy to identify (Figure 4A) since they have characteristic anti-phase-multiplet patterns (Bodenhausen et al., 1984b). The cross-peaks that do not coincide with the chemical shifts of peptide protons were identified as NOEs from thrombin alone [(d) above] (Figure 5). These peaks were also found in a NOESY spectrum of thrombin itself under a similar experimental condition (spectrum not shown). This NOESY spectrum of thrombin contained no cross-peaks at the chemical shifts of the hirudin peptides. We also acquired NOESY spectra of thrombin–peptide complexes with lower concentrations of hirudin peptides and a fixed concentration of

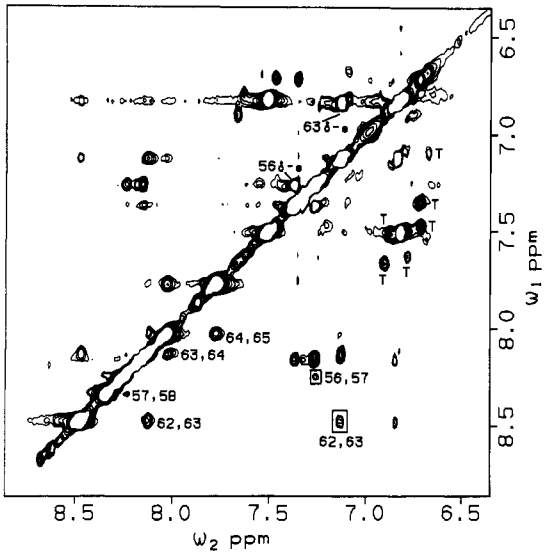

FIGURE 5: Transferred NH–NH NOE connectivities of HR2 extracted from the same NOESY spectrum shown in Figure 4B. The cross-peaks labeled with T were identified as arising from thrombin on the basis of a comparison with a NOESY spectrum of thrombin acquired under similar experimental conditions. The boxed cross-peaks are the transferred NOEs between the NH [Glu(57) and Glu(62)] and the δCH ring protons [Phe(56) and Tyr(63)] of the identified residues. Also indicated are the cross-peaks between the δCH and εCH ring protons of residues Phe(56) and Tyr(63).

thrombin. The NOE cross-peaks between protons on the peptides shown in Figures 4 and 5 decreased as the peptide-to-thrombin ratios became smaller (data not shown). Therefore, cross-peaks between peptide protons of residues Asp(55) to Gln(65) are dominated by transferred *intramolecular* NOEs since transferred peptide–protein NOEs have been observed to have an opposite dependence on the ratio of peptide and protein concentrations (James, 1976; Anglister et al., 1989).

In the previous sections, transferred NOEs have already been used to aid the sequential resonance assignments of hirudin peptides in solution (Figure 2). Most of the cross-peaks in Figure 4 represent intraresidue transferred NOEs as expected from the sequence-specific resonance assignments of the hirudin peptides (Table I). In Figure 5, a few more sequential transferred NOEs can be resolved and assigned. These include the NH–NH NOEs between residues Glu(57) and Glu(58), between residues Glu(62) and Tyr(63), between Tyr(63) and Leu(64), and between Leu(64) and Gln(65). There are also transferred NOEs between the δCH_2 ring protons of Phe(56) and the NH proton of Glu(57) and between the NH proton of residue Glu(62) and the δCH_2 ring protons of Tyr(63) (boxed cross-peaks in Figure 5).

Further identification of the following medium- and long-range transferred NOEs greatly facilitated the characterization of the thrombin-bound conformation of residues Phe(56) to Gln(65) of hirudin fragments. A weak NOE cross-peak corresponding to the resonance frequencies of the αCH proton of Glu(61) and the NH proton of Leu(64) was observed as indicated by the boxed cross-peak in Figure 2B. The same cross-peak also exists in the NOESY spectrum of thrombin interacting with peptide HR2 (spectrum not shown). Thrombin also induces NOEs between the αCH proton of Glu(61) and the side-chain protons of Leu(64) and between the αCH proton of Glu(62) and the γCH_2 protons of Gln(65) (Figure 4). Figure 6 displays another region of the NOESY spectrum of peptide HR2 in complex with thrombin. We see NOE cross-peaks between the side-chain protons of residues

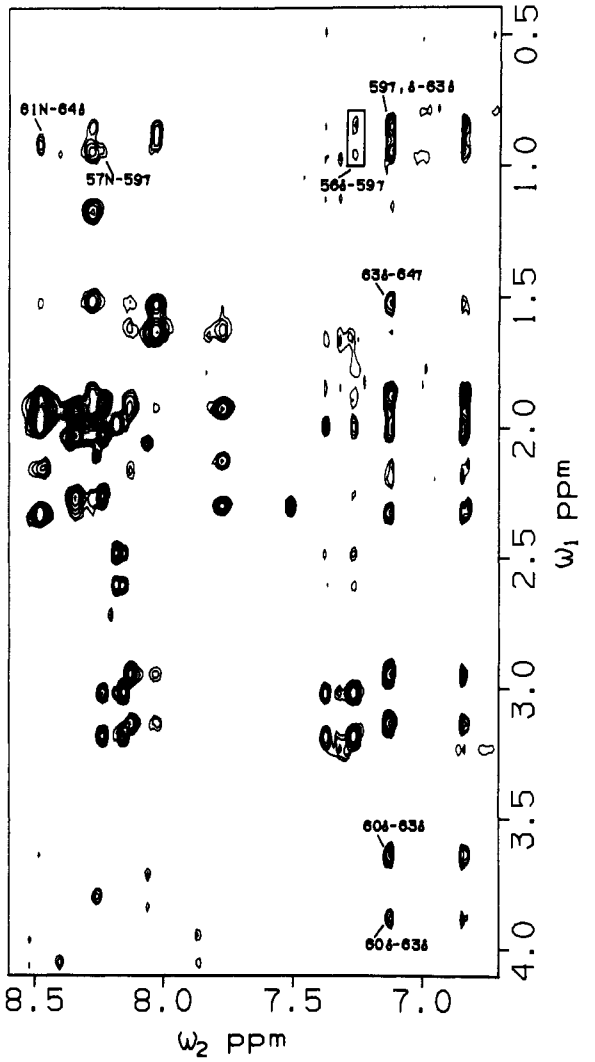

FIGURE 6: Another region of the NOESY spectrum (see also Figures 4B and 5) of HR2 complexed to thrombin. A few medium-range transferred NOEs are indicated by the residues involved. The label, 61N–64δ, for example, refers to an NOE between the NH proton of Glu(61) and the δCH_3 protons of Leu(64). The label 56δ–59γ indicates the NOE between the γCH_3 protons of Ile(59) and the δCH_2 ring protons of Phe(56) (small peak at the lower part of the box). Furthermore, these NOEs are extremely weak, but they were reproducible in several different NOESY experiments involving both peptides HR1 and HR2 (data not shown). As discussed in the text, the existence of NOEs between Phe(56) and Ile(59) can also be substantiated by the existence of an NOE between the γCH_3 protons of Ile(59) and the NH proton of Glu(57) (57N–59γ), which implies that the peptide backbone reverses at residues Glu(57) and Glu(58).

Ile(59) and Tyr(63), between those of residues Pro(60) and Tyr(63) and between residues Tyr(63) and Leu(64). Furthermore, there are NOEs between the NH proton of Glu(61) and the δCH_3 protons of Leu(64) and between the NH proton of Glu(57) and the γCH_3 protons of Ile(59).

Finally, there are small, but reproducible, cross-peaks corresponding to the chemical shifts of the δCH_2 protons of Phe(56) and the γCH_3 protons of Ile(59) (bottom peak in the small box in Figure 6) and the δCH_3 protons of Ile(59) and Leu(64) (peak at the top in the box). Since there is a resonance overlap between the δCH_3 protons of Ile(59) and the δCH_3 protons of Leu(64) (Table I), we assigned only one of the cross-peaks to the NOE interactions between the δCH_2 protons of Phe(56) and the γCH_3 protons of Ile(59). Table II represents a survey of all the sequential and medium-range transferred NOEs that characterize the backbone structure of hirudin peptides bound to thrombin.

Table II: Survey of the NMR Data of the C-Terminal Peptides of Hirudin[a]

Hirudin	52	53	54	55	56	57	58	59	60	61	62	63	64	65
Fragment	N	D	G	D	F	E	E	I	P	E	E	Y	L	Q
L_{NH}	x	-	-	-	w	s	s	s	s	w	s	s	s	s
$L_{\alpha H}$	-	-	-	w	s	s	s	s	s	s	s	s	s	s
L_{CH}	-	-	x	w	s	s	s	s	s	s	s	s	s	s
$d_{\alpha N}$	-	m	m	m	m	m	s	m[b]	s	m	m	m	m	m
$d_{\beta N}$	-	-	x	w	w	w	w	m[b]	w	w	w	w	w	w
d_{NN}	-	-	m	m	?	w	-	-	-	?	m	m	m	m
$d_{\alpha N}(i,i+3)$	-	?	-	-	-	x	-	-	-	w	-	x	x	x
$d_{\alpha\beta}(i,i+3)$	-	-	-	-	-	-	-	-	-	m	m[c]	x	x	x

[a] L_{NH}, $L_{\alpha H}$, and L_{CH}, line-broadening effects on the NH, αCH, and side-chain protons by thrombin binding; s, strong line broadening observed; w, weak line broadening observed; $d_{\alpha N}$, $d_{\beta N}$, and d_{NN}, $d_{\alpha N}(i,i+3)$, $d_{\alpha\beta}(i,i+3)$, sequential and medium-range NOEs between αCH, βCH, and NH protons; w, weak; m, medium; s, strong intensities of NOEs. In the table, a minus sign (-) indicated that an effect was not observed; x indicates that the NMR parameter is not applicable to that residue; and a question mark (?) indicates that the resonances could not be assigned because of spectral overlap with those from other residues. [b] For NOEs involving the proline residue, the δCH_2 protons are used in place of the NH protons of other residues. [c] This medium-range NOE pertains to that between the αCH proton of Glu(62) and the γCH_2 protons of Gln(65) (Figure 4).

Table III: Observed Transferred NOEs and Standard Distances between the Ring Protons of Pro(60) with Different Ring Conformations[a]

proton pair	d_{ru} (Å)	NOE	d_{rd} (Å)	NOE
αH–γCH^1	4.11	m*	4.05	m
αH–γCH^2	3.43	m	3.94	m
αH–δCH^1	3.98	w	4.06	w
αH–δCH^2	3.89	w	3.85	w
βH^1–δCH^1	3.25	m	3.85	w
βH^1–δCH^2	4.04	m*	4.12	w
βH^2–δCH^1	4.00	w	4.04	m*
βH^2–δCH^2	4.03	w	3.53	m

[a] d_{ru} (Å) and d_{rd} (Å) are the distances between the ring protons of Pro(60) in the "up" and "down" configurations, respectively. They were calculated from the standard geometry of the proline residue documented in the ECEPP/2 program (Némethy et al., 1983). For a carbon atom with two attached protons, a superscript over the hydrogen is used to distinguish them. NOE intensities are characterized in the same way as described in Table II. NOEs with an asterisk are a combination of direct NOE transfers and secondary spin-diffusion processes (see the text for details).

NOE Distance Constraints. To determine the thrombin-bound conformation of the C-terminal peptides of hirudin, it is necessary to convert the NOE information into interproton distance constraints (Table IV). We used intraresidue transferred NOEs of Pro(60) to correlate NOE intensities with interproton distances. Pro(60) takes on a trans conformation when the peptides bind to thrombin, as indicated by the NOEs between the αCH proton of Ile(59) and the δCH_2 protons of Pro(60) (Table II). Furthermore, with the trans ring conformation, there are so-called "up" and "down" configurations for the puckering of the Pro ring (Momany et al., 1975; Némethy et al., 1983). Table III represents a comparison of the observed transferred NOEs with the standard distances between the ring protons of Pro(60) in different puckering

configurations. The experimental data are more consistent with an "up" configuration for the ring of Pro(60) since the distances (4.05 and 3.94 Å) between the αCH proton and the γCH_2 protons for the "down" configuration are too large to give rise to NOEs of medium intensities. With the "up" configuration, an NOE of medium intensity should be observed for the interaction of the αCH proton with one of the well-resolved γCH_2 protons with a distance of 3.43 Å. An NOE of medium intensity was also observed for the interaction between the αCH proton and the second γCH_2 proton with a distance of 4.11 Å. This NOE presumably includes a secondary interaction (spin diffusion) involving the proton pairs separated by a distance of 3.43 Å ($\alpha H-\gamma CH^1$) and the γCH protons which are 1.75 Å from each other ($\gamma CH^1-\gamma CH^2$). A similar situation exists for the NOE interaction between the βCH and the δCH protons ($\beta CH^1-\delta CH^2$ and $\beta CH^2-\delta CH^1$ in Table III). However, spin diffusion is very limited in the transferred NOE spectra (200 ms mixing time) of the hirudin peptides. It may occur only between nearby protons (<2 Å apart) since, for example, no NOEs exist between the αCH proton and the γCH_2 protons of Ile(59) even though a relatively strong NOE is seen between the αCH proton and the δCH_3 protons (Figure 4).

The NOE intensities between the ring protons of Pro(60) (Table III) and between those of Phe(56) and Tyr(63) (Figure 5) were used as internal standards in the conversion of other observed NOEs into proton–proton distances. Thus, a weak NOE should correspond to an interproton distance between 3.8 and 4.2 Å. A medium NOE would be translated into a distance between 3.2 and 3.6 Å. The observation of a strong NOE between two protons suggests that these protons are less than 2.6 Å apart because the interactions of the δCH and εCH protons (2.5 Å) of both Phe(56) and Tyr(63) give rise to strong transferred NOE cross-peaks (Figure 5). This calibration procedure was considered satisfactory since it produced an upper bound of 3.6 Å for the distances, $d_{\alpha N}$, of all residues (Leach et al., 1977; Billeter et al., 1982). Table IV compiles the interproton distances for the hirudin peptides bound to thrombin. It should be noted that mainly upper bounds were determined from the observed NOEs: weak NOEs, 4.2 Å; medium NOEs, 3.6 Å; and strong NOEs, 2.8 Å. Upper bounds of 5 Å were assigned for NOEs involving side-chain protons to allow for the absence of stereospecific assignments. These include, for example, the distances between the γCH_3 and δCH_3 protons of Ile(59) and the ring protons of Tyr(63). The few lower bounds correspond to proton pairs that do not exhibit any transferred NOEs and that were consistently forced too close to each other during distance geometry calculations incorporating only upper bounds as constraints. The missing NOEs cannot be a result of very severe line broadening by thrombin binding since the involved protons exhibited all other expected NOEs (especially those from sequential interactions). Examples of these are the $\alpha CH-\gamma CH_2$ and the $\alpha CH-\delta CH_3$ proton pairs of Ile(59) (Figure 4) and the NH–NH proton pairs of Glu(58) and Ile(59) (Figure 5; Table II).

It has been shown previously that short distances (less than 4 Å), such as $d_{\alpha N}(i,i+3)$ and $d_{\alpha\beta}(i,i+3)$, are indicative of helical conformations of the involved amino acid residues (Wüthrich et al., 1984; Wagner et al., 1986; Wüthrich, 1986). The close proximity between the αCH proton of Glu(61) and the NH and βCH_2 protons of Leu(64) (Table IV) thus suggests that residues Glu(61), Glu(62), Tyr(63), and Leu(64) are involved in a helical structure in the cmplex. This is further supported by the short sequential distances, d_{NN}, from residues Glu(62) to Gln(65). The backbone conformation of residue Gln(65) may be distorted from that of an α-helix since the expected i-to-(i+3) NOE between the αCH proton of Glu(62) and the NH proton of Gln(65) was not observed (Figure 2B; Table II).

Table IV: Distance Constraints Derived from Transferred NOE Experiments[a]

	Upper Bounds (Å)
Asp(55)–Asp(55):	HN–HB 3.6
Phe(56)–Phe(56):	HN–HD2 3.6; HN–HB 3.6
Glu(57)–Glu(57):	HN–HB 3.6; HN–HG 3.6; HA–HG 3.6
Glu(58)–Glu(58):	HN–HB 3.6; HN–HG 3.6; HA–HG 3.6
Ile(59)–Ile(59):	HN–HB 3.6; HN–HG1 3.6; HN–HG2 3.6; HA–HG2 3.6
Glu(61)–Glu(61):	HN–HB 3.6; HN–HG 2.8; HA–HG 3.6
Glu(62)–Glu(62):	HN–HB 3.6; HN–HG 4.2; HA–HG 4.2
Tyr(63)–Tyr(63):	HN–HD1 3.6; HN–HB 3.6; HA–HD2 3.6
Leu(64)–Leu(64):	HN–HB 3.6; HN–HG 3.6; HN–HD1 3.6; HN–HD2 3.6; HA–HD2 2.8; HA–HD1 3.6
Gln(65)–Gln(65):	HN–HB 3.6; HN–HG 3.6; HA–HG 3.6
Asp(55)–Phe(56):	HA–HN 3.6; HB–HN 4.2; HN–HN 3.6
Phe(56)–Glu(57):	HD1–HN 4.2; HA–HN 3.6; HB–HN 4.2
Glu(57)–Glu(58):	HN–HN 4.2; HA–HN 3.6
Glu(58)–Ile(59):	HA–HN 2.8; HB–HN 3.6
Ile(59)–Pro(60):	HA–HD 3.6; HG2–HD 4.2
Pro(60)–Glu(61):	HA–HN 2.8
Glu(61)–Glu(62):	HA–HN 3.6; HB–HN 4.2
Glu(62)–Tyr(63):	HN–HN 3.6; HA–HN 3.6; HB–HN 4.2; HN–HD1 4.2; HB–HD2 3.6; HB–HE2 3.6
Tyr(63)–Leu(64):	HN–HN 3.6; HA–HN 3.6; HD1–HD1 4.2; HB–HN 4.2; HD1–HG 4.2
Leu(64)–Gln(65):	HN–HN 3.6; HA–HN 3.6; HD1–HN 4.2; HD2–HN 4.2; HB–HN 4.2
Glu(57)–Ile(59):	HN–HG2 4.2
Phe(56)–Ile(59):	HD1–HG2 5.0
Pro(60)–Tyr(63):	HG–HE1 5.0; HD–HD1 5.0
Glu(61)–Leu(64):	HA–HN 4.2; HN–HD1 4.2; HA–HB 3.6; HA–HD1: 3.6; HA–HG 3.6; HG–HD1 5.0
Glu(62)–Gln(65):	HA–HG 4.2
Ile(59)–Tyr(63):	HG2–HD1 5.0; HD1–HD1 5.0; HG2–HE1 5.0; HD1–HE1 5.0; HD1–HN 5.0; HD1–HB 5.0
	Lower Bounds (Å)
Ile(59)–Ile(59):	HA–HG1 4.0; HA–HD1 4.0
Glu(58)–Ile(59):	HN–HN 4.0; HN–HG2 4.0
Ile(59)–Pro(60):	HG1–HD 4.0
Glu(62)–Tyr(63):	HG–HE2 4.0; HG–HD2 4.0
Tyr(63)–Leu(64):	HB–HB 4.0; HD1–HB 4.0
Glu(57)–Ile(59):	HN–HG1 4.0
Pro(60)–Tyr(63):	HD–HB 4.0; HB–HB 4.0; HG–HB 4.0
Ile(59)–Tyr(63):	HB–HB 4.0; HG1–HB 4.0

[a] All distances were derived from the NOESY spectra of peptide HR2 in the presence of thrombin. The atom labels follow the convention adopted in the ECEPP/2 program (Némethy et al., 1983).

Three-Dimensional Structure of the Thrombin-Bound Peptides. On the basis of interproton distances, one can, in principle, determine the thrombin-bound structure of the binding sequence (55–65) of the hirudin peptides using a distance geometry algorithm (Braun & Gō, 1985). Structural calculations were carried out only for fragment 56–65 since no medium- or long-range NOEs were observed with residue Asp(55) (Tables II and IV). Upper bounds of 3.6 Å for all sequential distances, such as $d_{\alpha N}$, $d_{\beta N}$, and d_{NN}, are insufficient to define the local conformation of individual residues (Leach et al., 1977; Billeter et al., 1982). Distance geometry computations were carried out to generate two sets of conformations (Figure 7) of the terminally blocked decapeptide (*N*-acetyl-Phe-Glu-Glu-Ile-Pro-Glu-Glu-Tyr-Leu-Gln-NHMe) that were free of steric overlaps and that were consistent with the input interproton distances (Table IV). For these computations, a contact energy of 10 kcal/mol was first used to define steric overlaps (Vásquez & Scheraga, 1988). Distance constraints were incorporated sequentially and one pair of distances at a time (Braun & Gō, 1985) starting from sets of

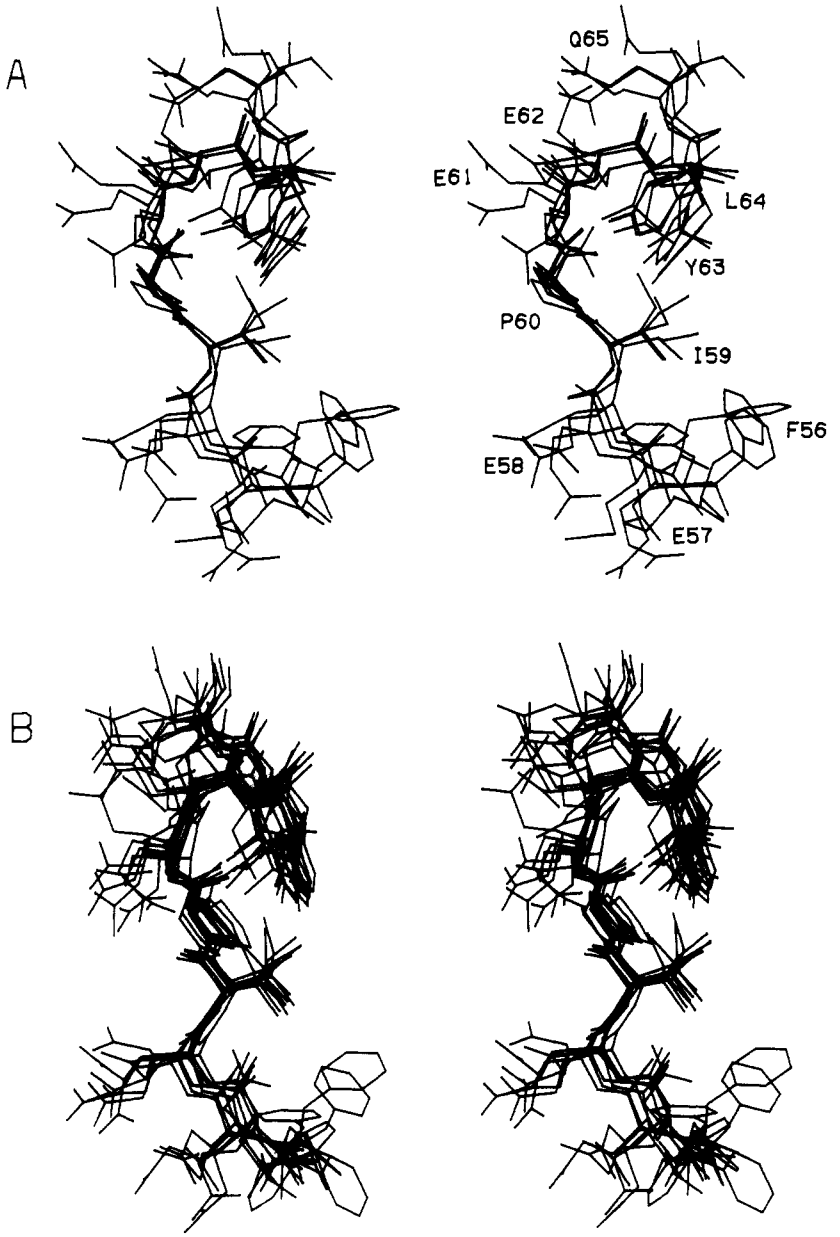

FIGURE 7: Comparison of structures of residues Phe(56) to Gln(65) of hirudin peptides on the basis of NOE-constrained molecular modeling (see text). (A) Structures generated by a preliminary distance geometry calculation based on random sampling. (B) Refined structures computed by restricting the sampling region of the dihedral angles of each residue to that determined from the structures in (A). It should be noted that the NMR structures are not unique in that there are large variations in the atomic coordinates of various converged conformations.

initial structures, randomly sampled either from the single-residue backbone dihedral angle distributions (Zimmerman et al., 1977; Vásquez & Scheraga, 1988) or from certain predefined regions (see the following sections) in the ϕ–ψ map for each residue (Zimmerman et al., 1977). Structures with values of the distance part of the objective function less than 1.0 were selected, and these were then subjected to a second optimization, using a contact energy of 5 kcal/mol with up to four pairs of distance constraints incorporated at a time. Finally, a contact energy of 3 kcal/mol was used in the optimization incorporating all the distance constraints at once. Structures thus generated were checked for the satisfaction of input distance information by use of two criteria: a structure should have the value of the distance part of the objective function less than 1.0 (criterion of convergence) and all distance violations should be less than 0.5 Å (criterion for goodness of fit).

In the first set of computations, a total of 5 converged structures were found starting with 400 initial conformations sampled on the basis of the single-residue distributions. Among the 5 structures, one contained a residue [Glu(57)] with the backbone conformation in the positive ϕ region of the ϕ–ψ conformational map (Zimmerman et al., 1977). This structure was eliminated since a positive value of ϕ is not favorable for amino acid residues other than a Gly or an Ala (Zimmerman et al., 1977; Némethy & Scheraga, 1977; Richardson, 1981; Iijima et al., 1987). The rest of the structures were then superimposed by using the α-carbon atoms of residues Ile(59) to Gln(65). The peptide backbone of residues Glu(58) to Ile(59) is well-defined by the NOE distance constraints (Figure 7A). Especially, the residues Glu(61) to Gln(65) are in a helical structure although the backbone ϕ–ψ angles of individual residues deviate significantly from those (ϕ, −60°; ψ, −40°) of an α-helix. Furthermore, the relative positions of the side chains of residues Ile(59), Pro(60), Tyr(63), and Leu(64) remain the same in all four structures. There is, however, a large variation in the structure of residues Phe(56) and Glu(57), as one may expect from the very few NOE

constraints involving these two residues (Table IV).

To refine the structure further, the second set of conformations was computed starting from 400 initial structures *uniformly* sampled from regions (A, G, C, or E) of the ϕ–ψ map for each residue in Figure 7A. Thus, backbone conformations of residues Glu(61) to Gln(65) were restricted within the helical or the A region (ϕ, −110° to −40°; ψ, −90° to −10°) (Zimmerman et al., 1977). Sampling for residues Glu(57), Glu(58), Ile(59), and Pro(60) was restricted within the G (ϕ, −180° to −110°; ψ, −90° to −40°), the C (ϕ, −110° to −40°; ψ, 50–130°), the E (ϕ, −180° to −110°; ψ, 110–220°), and the C (ϕ, −110° to −40°; ψ, 50–130°) regions, respectively. Sampling of Phe(56), however, was still based on the single-residue backbone dihedral angle distributions due to the large variation in the backbone conformation of this residue (Figure 7A). A total of 11 structures converged in this second set of distance geometry computations. Again, one structure was eliminated that contained a residue [Phe(56)] with the backbone conformation in the positive ϕ region of the ϕ–ψ map. Figure 7B displays a best superposition of eight representative structures. The backbone conformations of residues Glu(57) to Gln(65) is better defined than those for the structures displayed in Figure 7A. There is a hydrophobic cluster formed by the nonpolar side chains of residues Ile(59), Pro(60), Tyr(63), and Leu(64). This hydrophobic core is brought about by an extended structure involving residues Ile(59) and Pro(60) and by a one and a half turn of slightly distorted α-helix with hydrogen bonds between the carbonyl oxygen of Pro(60) and the amide NH protons of Tyr(63) and/or Leu(64) and between the carbonyl oxygen of Glu(61) and the NH proton of Gln(65). There is also a chain reversal at residues Glu(57) and Glu(58) such that the phenyl ring of Phe(56) bends back to form a continuous hydrophobic surface with the side chains of residues Ile(59), Pro(60), Tyr(63), and Leu(64).

Discussion

The structure–function relationship of the C-terminal fragments of hirudin has been extensively studied by Krstenansky and co-workers (Krstenansky & Mao, 1987; Krstenansky et al., 1987, 1988a,b; Mao et al., 1988). It was proposed that a hinged α-helix may exist in the region of residues Asp(55) to Gln(65). This helical structure has an amphiphilic feature; namely, one side of the helix is enriched by hydrophilic residues of Asp(55), Glu(57), Glu(58), Glu(61), Glu(62), and Gln(65) and the other side by hydrophobic residues of Phe(56), Ile(59), Pro(60), Tyr(63), and Leu(64). Analogues of fragment 55–65 were synthesized in which each residue was replaced by an Ala one by one. Peptides with an Ala at positions 56, 57, 59, 60, and 64, respectively, lost inhibitory activity, indicating that the essential residues are Phe(56), Glu(57), Ile(59), Pro(60), and Leu(64). These residues, except for Glu(57), are all located on one side of the putative helical structure. Furthermore, inhibitory activities were observed for the peptides containing a disulfide bond with a D-Cys at position 58 and an L-Cys at position 61 or with a D-Cys at position 60 and an L-Cys at position 63. However, an analogue in which Glu(58) was replaced by a Pro also retained inhibitory activity. Since Pro is a strong helix breaker, an α-helix is unlikely at least within the N-terminal residues Asp(55) to Pro(60) of the fragment.

Transferred NOE data obtained in this study (Tables II and IV) indicate that residues 55–65 of hirudin fragments take on a well-defined structure when bound to thrombin. This is particularly true for residues Phe(56) to Gln(65) since various medium- or long-range transferred NOEs were observed between the backbone and side-chain protons of these residues. It is interesting that the distance geometry structures of the fragment 56–65 are still amphiphilic in that one side of the molecule is polar and charged and the other side is hydrophobic (Figure 7). The phenyl ring of Phe(56) is brought back by a chain reversal at residues Glu(57) and Glu(58) to form a hydrophobic cluster with the side chains of residues Ile(59), Pro(60), Tyr(63), and Leu(64). There is a slightly distorted α-helix within residues Glu(61) and Gln(65) with hydrogen bonds between the carbonyl oxygen of Pro(60) and the amide NH protons of Tyr(63) and/or Leu(64) and between the carbonyl oxygen of Glu(61) and the NH proton of Gln(65). Residues Glu(58), Ile(59), and Pro(60), on the other hand, are in extended conformations. Nevertheless, the α-carbons of Pro(60) and Tyr(63) are close enough (less than 7 Å) to accommodate a disulfide bond between the two residues. The distance between the α-carbon atoms of residues Glu(58) and Glu(61) is larger than 7 Å, but the orientation of their side chains may still allow a disulfide bridge with a D-Cys at position 58 and an L-Cys at position 61. It should also be noted that the backbone conformations of residues Glu(58) and Pro(60) are very similar in all of the computed structures based on NOE constraints (Figure 7B). The replacement of Glu(58) by a Pro may further stabilize the thrombin-bound conformation of hirudin peptides. This may explain why an analogue in which Glu(58) was replaced by a Pro showed higher inhibitory activity (Krstenansky et al., 1988b).

In previous studies, it was found that the C-terminal fragment of hirudin does not inhibit the proteolysis of tripeptide chromogenic substrates catalyzed by low concentrations of thrombin (Krstenansky & Mao, 1987). In order to examine the possibility that the C-terminal fragment of hirudin may bind to the active site of thrombin under the conditions under which the NMR observations were made, experiments were also carried out with a modified thrombin in which the active site was blocked irreversibly with PPACK (Kettner & Shaw, 1979). We found that the derivatized thrombin induces similar transferred NOEs and line broadening (see the next section) in the hirudin peptides as active thrombin. Thus, the C-terminal peptides of hirudin do not bind to the catalytic site of thrombin.

As reported in our previous studies, differential line broadening of peptide resonances is useful to identify the residues of peptides interacting with thrombin (Ni et al., 1989a,b). Thus, the residues Asn(52), Asp(53), and Gly(54) of the C-terminal peptides of hirudin are not directly involved in the interaction with thrombin because of the lack of line broadening (Table II). This conclusion is consistent with the previous finding that these residues contribute very little to the potency of the C-terminal peptides of hirudin in the inhibition of thrombin (Krstenansky et al., 1987; Mao et al., 1988). The observation that the side-chain proton resonances of Phe(56), Ile(59), Tyr(63), and Leu(64) are significantly broadened by thrombin binding provides further support to the conclusion that nonpolar residues in the C-terminal fragment of hirudin are important in the interaction with thrombin. The side chains of residues Ile(59), Pro(60), Tyr(63), and Leu(64) form a continuous hydrophobic surface with the phenyl ring of residue Phe(56) (Figure 7). Assuming that this hydrophobic surface is part of the binding site with thrombin, the three Glu residues, Glu(58), Glu(61), and Glu(62), would all point away into the solvent. This may explain why these Glu residues are not important in the binding of hirudin peptides to thrombin (Krstenansky et al., 1987). Furthermore, since the side chain of Glu(57) can be very close

to the hydrophobic core, there may be specific ionic interactions (ion pairs) between Glu(57) and positively charged residues on thrombin (Stone et al., 1987; Chang, 1989). This may be the reason why only Glu(57) of all the polar residues is important in the binding of hirudin peptides to thrombin (Krstenansky et al., 1987). It was recently found that the sulfonation of Tyr(63) increased the inhibitory activity of the C-terminal peptides of hirudin (Maraganore et al., 1989). There may be other positively charged residues on thrombin which would interact with the negative charge introduced to Tyr(63) by sulfonation.

CONCLUSION

The solution conformation of the C-terminal fragments of hirudin has been examined by use of NMR spectroscopy. Measurements of line broadening and transferred NOEs indicated that residues Asp(55) to Gln(65) of hirudin peptides are important in the interaction with thrombin. These peptides take on a well-defined structure only when bound to thrombin. The structure of the fragment 56–65 of hirudin has been characterized by distance geometry calculations incorporating distance constraints derived from transferred NOEs. There is, on one side of the molecule, a continuous hydrophobic surface formed by the nonpolar side chains of residues Phe(56), Ile(59), Pro(60), Tyr(63), and Leu(64) and, on the other, a polar and charged surface where all other residues are located. This structural feature is brought about by a chain reversal at residues Glu(57) and Glu(58), by an extended structure involving residues Ile(59) and Pro(60), and by a one and a half turn of slightly distorted α-helix from residues Glu(61) to Gln(65). The structure of the thrombin-bound C-terminal peptides of hirudin may provide a basis for the design of specific thrombin inhibitors.

ADDED IN PROOF

After the revised manuscript of this paper was returned to the editorial office, we were informed that the crystal structure of the complex of intact hirudin with human thrombin has been determined and refined to high resolution (2.3 Å) (Rydel et al., 1990). A preliminary comparison revealed that both the NMR and X-ray results are consistent with each other. Furthermore, the electron density of residues Asn(52), Asp(53), and Gly(54) of hirudin was found to be poorly defined in the complex, in agreement with our conclusion that these residues are not involved in binding to thrombin since no thrombin-induced line broadening was observed for the NH and side-chain protons of these residues.

ACKNOWLEDGMENTS

We thank Jean Lefebvre for peptide synthesis and Steve Thomas for help in setting up the distance geometry program on the Intel computer. We also thank Dr. E. O. Purisima for discussions and help with computer graphics and Dr. A. C. Storer for his support of this project.

REFERENCES

Albrand, J. P., Birdsall, B., Feeney, J., Roberts, G. C. K., & Burgen, A. S. V. (1979) *Int. J. Biol. Macromol. 1*, 37.

Anglister, J., Levy, R., & Scherf, T. (1989) *Biochemistry 28*, 3360.

Aue, W. P., Bartholdi, E., & Ernst, R. R. (1976) *J. Chem. Phys. 64*, 2229.

Bagdy, D., Barabas, E., Gráf, L., Petersen, T. E., & Magnusson, S. (1976) *Methods Enzymol. 45*, 669.

Balaram, P., Bothner-By, A. A., & Dadok, J. (1972) *J. Am. Chem. Soc. 94*, 4015.

Bax, A., & Davis, D. G. (1985a) *J. Magn. Reson. 63*, 207.

Bax, A., & Davis, D. G. (1985b) *J. Magn. Reson. 65*, 355.

Billeter, M., Braun, W., & Wüthrich, K. (1982) *J. Mol. Biol. 155*, 321.

Bodenhausen, G., Kogler, H., & Ernst, R. R. (1984a) *J. Magn. Reson. 58*, 370.

Bodenhausen, G., Wagner, G., Rance, M., Sorensen, O. W., Wüthrich, K., & Ernst, R. R. (1984b) *J. Magn. Reson. 59*, 542.

Bothner-By, A. A., Stephens, R. L., Lee, Ju-mee, Warren, C. D., & Jeanloz, R. W. (1984) *J. Am. Chem. Soc. 106*, 811.

Braun, P. J., Dennis, S., Hofsteenge, J., & Stone, S. R. (1988) *Biochemistry 27*, 6517.

Braun, W., & Gō, N. (1985) *J. Mol. Biol. 186*, 611.

Braunschweiler, L., & Ernst, R. R. (1983) *J. Magn. Reson. 53*, 521.

Chang, J.-Y. (1983) *FEBS Lett. 164*, 307.

Chang, J.-Y. (1986) *Biochem. J. 240*, 797.

Chang, J.-Y. (1989) *J. Biol. Chem. 264*, 7141.

Clore, G. M., & Gronenborn, A. M. (1982) *J. Magn. Reson. 48*, 402.

Clore, G. M., Sukumaran, D. K., Nilges, M., Zarbock, J., & Gronenborn, A. M. (1987) *EMBO J. 6*, 529.

Degryse, E., Acker, M., Defreyn, G., Bernat, A., Maffrand, J. P., Roitsch, C., & Courtney, M. (1989) *Protein Eng. 2*, 459.

Dodt, J., Müller, H.-P., Seemüller, U., & Chang, J.-Y. (1984) *FEBS Lett. 165*, 180.

Dodt, J., Seemüller, U., & Fritz, H. (1987) *Biol. Chem. Hoppe-Seyler 368*, 1447.

Dodt, J., Köhler, S., & Baici, A. (1988) *FEBS Lett. 229*, 87.

Eich, G., Bodenhausen, G., & Ernst, R. R. (1982) *J. Am. Chem. Soc. 104*, 3731.

Fenton, J. W., II (1981) *Ann. N.Y. Acad. Sci. 370*, 468.

Folkers, P. J. M., Clore, G. M., Driscoll, P. C., Dodt, J., Köhler, S., & Gronenborn, A. M. (1989) *Biochemistry 28*, 2601.

Gilboa, N., Villannueva, G. B., & Fenton, J. W., II (1988) *Enzyme 40*, 144.

Haruyama, H., & Wüthrich, K. (1989) *Biochemistry 28*, 4301.

Haruyama, H., Qian, Y.-Q., & Wüthrich, K. (1989) *Biochemistry 28*, 4312.

Iijima, H., Dunbar, J. B., Jr., & Marshall, G. R. (1987) *Proteins 2*, 330.

James, T. L. (1976) *Biochemistry 15*, 4724.

Jeener, J., Meier, B. H., Bachmann, P., & Ernst, R. R. (1979) *J. Chem. Phys. 71*, 4546.

Kaiser, B., Hauptmann, J., Weiss, A., & Markwardt, F. (1985) *Biomed. Biochim. Acta 7*, 1201.

Kessler, H., Griesinger, C., Kerssebaum, R., Wagner, K., & Ernst, R. R. (1987) *J. Am. Chem. Soc. 109*, 607.

Kettner, C., & Shaw, E. (1979) *Thromb. Res. 14*, 969.

Kikumoto, R., Tamao, Y., Tezuka, T., Tonomura, S., Hara, H., Ninomiya, K., Hijikata, A., & Okamoto, S. (1984) *Biochemistry 23*, 85.

Kobayashi, S., Kitani, M., Yamaguchi, S., Suzuki, T., Okada, K., & Tsunematsu, T. (1987) *Thromb. Haemostasis 53*, 305.

Konishi, Y., Kotts, C. E., Bullock, L. D., Ton, J. S., & Johnson, D. A. (1989) *Biochemistry 28*, 8872.

Krstenansky, J. L., & Mao, S. J. T. (1987) *FEBS Lett. 211*, 10.

Krstenansky, J. L., Owen, T. J., Yates, M. T., & Mao, S. J. T. (1987) *J. Med. Chem. 30*, 1688.
Krstenansky, J. L., Owen, T. J., Yates, M. T., & Mao, S. J. T. (1988a) *Biochim. Biophys. Acta 957*, 53.
Krstenansky, J. L., Owen, T. J., Yates, M. T., & Mao, S. J. T. (1988b) *Thromb. Res. 52*, 137.
Laskowski, M., Jr., & Kato, I. (1980) *Annu. Rev. Biochem. 49*, 593.
Leach, S. J., Némethy, G., & Scheraga, H. A. (1977) *Biochem. Biophys. Res. Commun. 75*, 207.
Lundblad, R. L. (1971) *Biochemistry 10*, 2501.
Macura, S., & Ernst, R. R. (1980) *Mol. Phys. 41*, 95.
Mao, S. J. T., Yates, M. T., Owen, T. J., & Krstenansky, J. L. (1988) *Biochemistry 27*, 8170.
Maraganore, J. M., Chao, B., Joseph, M. L., Jablonski, J., & Ramachandran, K. L. (1989) *J. Biol. Chem. 264*, 8692.
Marion, D., & Wüthrich, K. (1983) *Biochem. Biophys. Res. Commun. 113*, 967.
Markwardt, F. (1970) *Methods Enzymol. 19*, 924.
Markwardt, F., Hauptmann, J., Nowak, G., Klessen, C., & Walsmann, P. (1982) *Thromb. Haemostasis 47*, 226.
Markwardt, F., Fink, G., Kaiser, B., Klöcking, H.-P., Nowak, G., Richter, M., & Strürzebecher, J. (1988) *Pharmazie 43*, 202.
Momany, F. A., McGuire, R. F., Burgess, A. W., & Scheraga, H. A. (1975) *J. Phys. Chem. 79*, 2361.
Némethy, G., & Scheraga, H. A. (1977) *Q. Rev. Biophys. 10*, 239.
Némethy, G., Pottle, M. S., & Scheraga, H. A. (1983) *J. Phys. Chem. 87*, 1883.
Ni, F., Scheraga, H. A., & Lord, S. T. (1988) *Biochemistry 27*, 4481.
Ni, F., Konishi, Y., Bullock, L. D., Rivetna, M. N., & Scheraga, H. A. (1989a) *Biochemistry 28*, 3106.
Ni, F., Konishi, Y., Frazier, R. B., Scheraga, H. A., & Lord, S. T. (1989b) *Biochemistry 28*, 3082.
Ni, F., Meinwald, Y. C., Vásquez, M., & Scheraga, H. A. (1989c) *Biochemistry 28*, 3094.
Otting, G., Widmer, H., Wagner, G., & Wüthrich, K. (1986) *J. Magn. Reson. 66*, 187.
Plateau, P., & Guéron, M. (1982) *J. Am. Chem. Soc. 104*, 7310.
Rance, M. (1987) *J. Magn. Reson. 74*, 557.
Redfield, A. G., & Kuntz, S. D. (1975) *J. Magn. Reson. 19*, 250.
Richardson, J. S. (1981) *Adv. Protein Chem. 34*, 167.
Rydel, T. J., Ravichandran, K. G., Tulinsky, A., Bode, W., Huber, R., Fenton, J. W., II, & Roitsch, C. (1990) *Science* (submitted for publication).
Stone, S. R., & Hofsteenge, J. (1986) *Biochemistry 25*, 4622.
Stone, S. R., Braun, P. J., & Hofsteenge, J. (1987) *Biochemistry 26*, 4617.
Strürzebecher, J., Markwardt, F., Voigt, B., Wagner, G., & Walsmann, P. (1983) *Thromb. Res. 29*, 635.
Sukumaran, D. K., Clore, G. M., Preuss, A., Zarbock, J., & Gronenborn, A. M. (1987) *Biochemistry 26*, 333.
Vásquez, M., & Scheraga, H. A. (1988) *J. Biomol. Struct. Dyn. 5*, 757.
Wagner, G. (1983) *J. Magn. Reson. 55*, 151.
Wagner, G., Neuhaus, D., Wörgötter, E., Vasak, M., Kagi, J. H. R., & Wüthrich, K. (1986) *J. Mol. Biol. 187*, 131.
Walsmann, P., & Markwardt, F. (1981) *Pharmazie 36*, 653.
Wider, G., Hosur, R. V., & Wüthrich, K. (1983) *J. Magn. Reson. 52*, 130.
Wider, G., Macura, S., Kumar, A., Ernst, R. R., & Wüthrich, K. (1984) *J. Magn. Reson. 56*, 207.
Winzor, D. J., & Scheraga, H. A. (1964) *Arch. Biochem. Biophys. 104*, 202.
Wüthrich, K. (1986) *NMR of Proteins and Nucleic Acids*, Wiley & Sons, New York.
Wüthrich, K., Billeter, M., & Braun, W. (1984) *J. Mol. Biol. 180*, 715.
Zimmerman, S. S., Pottle, M. S., Némethy, G., & Scheraga, H. A. (1977) *Macromolecules 10*, 1.
Zuiderweg, E. R. P. (1987) *J. Magn. Reson. 71*, 283.